Received 20 July 2023, accepted 6 August 2023, date of publication 17 August 2023, date of current version 24 August 2023.

Digital Object Identifier 10.1109/ACCESS.2023.3305926

RESEARCH ARTICLE

Attitude Synchronization of Rigid Bodies With Event-Triggered Communication

JUAN R. AYALA-OLIVARES[1], ROGERIO ENRÍQUEZ-CALDERA[1], J. FERMI GUERRERO-CASTELLANOS[2], (Member, IEEE), AND SYLVAIN DURAND[3]

[1]Coordinación de Electrónica, Instituto Nacional de Astrofísica, Óptica y Electrónica, Puebla 72840, Mexico
[2]Facultad de Ciencias de la Electrónica, Benemérita Universidad Autónoma de Puebla (BUAP), Puebla 72570, Mexico
[3]CNRS, INSA Strasbourg, ICube UMR 7357, Strasbourg University, 67000 Strasbourg, France

Corresponding authors: Juan R. Ayala-Olivares (jrayala@inaoe.mx) and J. Fermi Guerrero-Castellanos (fermi.guerrero@correo.buap.mx)

This work was supported in part by the Doctoral CONAHCYT Scholarship under Grant 546826, in part by the Basic Science CONAHCYT Project under Grant CB-2015-257985, in part by the French-Mexican TOBACCO Project funded by the FORDECYT-PRONACES through the Joint SEP-CONAHCYT-ANUIESECOS Nord Program under Grant MX-296702 & FR-M18M02, and in part by the dark-NAV Project funded by the French National Research Agency under Grant ANR-20-CE33-0009.

ABSTRACT This article addresses the challenge of attitude synchronization of a group of rigid bodies (considered to be agents) with zero final angular velocity. A collaborative control strategy is proposed to tackle this issue, using decentralized consensus within a leader-follower scheme, and the communication between agents is activated by events. The attitude is parameterized by the unit quaternion. The control law incorporates an event function specifying the moment when the i-th agent should transmit attitude and angular velocity information to its neighbors. The communication topology between agents is modeled using a connected and undirected graph. The event-triggered communication produces asynchronous information exchange, reducing data traffic without compromising system performance. Furthermore, in practical scenarios such as networks of satellites or aerial robots, the proposed strategy could reduce the use of communication channel bandwidth. The Lyapunov method is utilized to analyze the stability of the overall system. Numerical simulation results confirm the proposal's effectiveness.

INDEX TERMS Attitude synchronization, cooperative control, consensus, control theory, event-based control, nonlinear control, rigid body dynamics.

NOMENCLATURE

$\mathbb{R}^n$	n-dimensional Euclidean space.
$\|\cdot\|$	Euclidean norm of a vector or induced Euclidean norm of a matrix.
$\mathbb{Q}$	Set of all quaternions.
$\mathbb{Q}_u$	Set of all unit quaternions $\mathbb{Q}_u = \{\mathbf{Q} \mid \mathbf{Q} \in \mathbb{Q}, \|\mathbf{Q}\| = 1\}$.
$\mathbf{Q}$	Unit quaternion $\mathbf{Q} = [q\ \mathbf{q}]^T$.
q	The scalar part of the quaternion $\mathbf{Q}$.
$\mathbf{q}$	The vector part of quaternion $\mathbf{Q}$.
$\hat{\mathbf{e}}$	Unit vector.
β	Rotation angle about $\hat{\mathbf{e}}$.
$(\cdot)^*$	Quaternion conjugate $\mathbf{Q}^* = [-q\ \mathbf{q}]^T$.
$(\cdot)^{-1}$	Quaternion inverse, for $\mathbf{Q} \in \mathbb{Q}_u$, $\mathbf{Q}^{-1} = \mathbf{Q}^*$.
$[x^\times]$	Skew-symmetric matrix associated to $x = [x_1\ x_2\ x_3]^T \in \mathbb{R}^3$. $[x^\times] = \begin{bmatrix} 0 & -x_3 & x_2. \\ x_3 & 0 & -x_1. \\ -x_2 & x_1 & 0 \end{bmatrix} \in \mathbb{R}^{3\times 3}$.
$\odot$	Quaternion product, for $\mathbf{Q}_i, \mathbf{Q}_j \in \mathbb{Q}_u$. $\mathbf{Q}_i \odot \mathbf{Q}_j := \begin{pmatrix} q_i & -\mathbf{q}_i^T. \\ \mathbf{q}_i & \mathbf{I}_3 q_i + [\mathbf{q}_i^\times] \end{pmatrix} \begin{pmatrix} q_j \\ \mathbf{q}_j \end{pmatrix}$
$\otimes$	Quaternion product 2 $\mathbf{Q}_i \otimes \mathbf{Q}_j := \mathbf{Q}_j \odot \mathbf{Q}_i$.
$\mathbf{E}^f$	Inertial coordinate frame $\mathbf{E}^f = [\hat{\mathbf{e}}_1^f, \hat{\mathbf{e}}_2^f, \hat{\mathbf{e}}_3^f]$.
$\mathbf{E}^i$	i-th rigid body coordinate frame $\mathbf{E}^i = [\hat{\mathbf{e}}_1^i, \hat{\mathbf{e}}_2^i, \hat{\mathbf{e}}_3^i]$.
$\mathbf{Q}_i$	The attitude of $\mathbf{E}^i$ relative to $\mathbf{E}^f$.
$\boldsymbol{\omega}_i$	The angular velocity of $\mathbf{E}^i$ relative to $\mathbf{E}^f$.
$\mathbf{Q}_i^m$	The attitude of $\mathbf{E}^i$ relative to $\mathbf{E}^f$ last time there was an event.
$\boldsymbol{\omega}_i^m$	Angular velocity last time there was an event.
$\mathbf{I}_3$	Identity matrix of dimension 3.

The associate editor coordinating the review of this manuscript and approving it for publication was Faissal El Bouanani.

$\mathbf{J}_i$	Inertia matrix of the i-th rigid body.
$\mathbf{\Gamma}_i$	Control input vector of the i-th rigid body.
$\mathbf{\Gamma}_i^d$	Disturbance vector of the i-th rigid body.
K_0^p, D_i, α_i	Control gains.
$\mathbf{Q}_d$	The reference (desired) attitude.
$\tilde{\mathbf{Q}}_i$	Relative attitude between $\mathbf{Q}_i$ and $\mathbf{Q}_d$.
$\mathbf{Q}_{ij}$	Relative attitude between $\mathbf{Q}_i$ and $\mathbf{Q}_j$.
$\mathbf{Q}_{ij}^m$	Relative attitude between $\mathbf{Q}_i^m$ and $\mathbf{Q}_j^m$.
$\mathbf{Q}_i^e$	Relative attitude between $\mathbf{Q}_i^m$ and $\mathbf{Q}_i$.

I. INTRODUCTION

Recently, Cyber-Physical Systems (CPS) have attracted the interest of the scientific and engineering community in the fields of embedded systems, communications, and automatic control [1]. CPS is a fusion of computing systems and physical elements interconnected by communication networks. Multi-agent systems (MAS) are a particular case of CPS, consisting of a network of dynamic systems that interact and communicate to achieve a group objective collaboratively. Collaboration and coordination enable the systems to do tasks that would be impossible to perform individually [2], [3]. Examples of such behavior in nature can be found in insects, birds, and fishes [4]. It is precisely inspired in nature, that coordination and cooperative control of MAS is of enormous interest, mainly when the group of agents is formed by a network of mobile autonomous systems for applications such as environmental mapping, monitoring, scientific exploration, load transportation, surveillance, and rescue. Such agents can be unmanned aerial vehicles (UAVs) [5], [6], unmanned ground vehicles (UGVs) [6], [7], unmanned underwater vehicles (UUVs) [8], or even a group of spacecrafts [9], satellites, and robot manipulators [10]. These systems fall into the framework of rigid bodies, where attitude synchronization is important and whose responsibility resides in a low-level controller [11], [12], [13].

Generally, two approaches have been adopted for coordinating multiple agents: centralized and distributed control. In centralized control, all computations and controls are driven by a central computer, which may result in high computational load memory requirement and communication bandwidth [14], [15]. On the other hand, it is often desirable to have individual control laws that are distributed (decentralized) that allow fundamental insights and scalability. Distributed coordination/cooperative control uses local interactions between agents to conduct collective behaviors of multiple agents and, therefore, to better achieve global missions [16], [17]. Decentralized cooperative control of MAS has captivated interest since it provides an effective solution for large-scale system control, simultaneously decreasing the complexity and computational load required for real-time implementations [3]. However, consensus and synchronization can be found among the different cooperative control problems. Furthermore, of particular interest is the control of a MAS, where a virtual leader is responsible for dictating the reference signals for the group through information exchange with only one other of the agents in the set. This problem is known as leader-follower consensus [18].

Leader-follower consensus and attitude synchronization among all the constituents of MAS is a fundamental problem in systems whose mathematical model falls within the framework of rigid bodies (RB). The objective of the latest is to drive all RB, also generally referred to as a group of agents, to the same attitude [19], [20], [21]. All previously described wealth of knowledge has motivated further exploration of the potential benefits of employing multiple inexpensive, straightforward RB operating collaboratively, *e.g.,* for advancing space-based interferometry and related applications, enabling the realization of complex missions previously constrained by individual spacecraft's limitations. Consequently, cooperative attitude control of multiple agents and, in particular, consensus and leader-follower consensus attitude, including small satellite networks [22] and fractionated spacecraft [23], has emerged as a promising avenue, offering cost-effectiveness, simplicity, and enhanced operational capabilities.

In the case of an RB network, a wireless communication network is employed to transmit control signals and data acquisition between agents. This means that information flow can increase drastically when all agents share a common channel. Additionally, in the spacecraft case, the performance is limited by energy availability and large intercommunication distances [24]. Therefore, when developing collaborative control algorithms, the effectiveness of communication and control should be considered [25]. An enormous challenge in the existing state of the art is the control paradigm used to share information among agents in a network that guarantees stability properties. The literature reports results from two different perspectives: reducing each transmission's size and the number of transmissions. The most commonly used methods are quantization techniques [26], [27], [28] and event-triggered techniques [29], [30], [31], [32], [33].

The event-triggered control (ETC) technique computes and updates the control signals only when a specific condition is satisfied. Typical mechanisms of event-based communication rely on functions that depend on the variation of the system state and/or the desired system output and whether the control signal should be updated or not [34], [35], [36], [37]. An excellent overview and bibliometric analysis of ETC are reported in [38]. In the framework of cooperative control of linear MAS, an event-triggered cooperative control allows sharing of information among the agents only when necessary and without sacrificing performance [39], [40], [41], [42]. The literature has examined several event function types, including state-based, time-based, and input-based events. Time-based events trigger an event at specific times or intervals. Input-based events depend on the control signal being used. Hybrid or mixed event-timed-driven coordination, in which events may be triggered by both state and time events, has also been scrutinized [42]. State-based events trigger an event when the error between the actual state and the state currently used by the controller surpasses a specific

threshold. This gives two main advantages: first, it is easy to implement due to its simplicity, and second the Zeno effect can be ruled out due to the minimum amount of time the error signal takes from going to zero to reaching a constant threshold [40].

Building upon the existing body of knowledge on the consensus of MAS under the leader-follower scheme, as established in the classical works by Ren and Beard [19] and Abdessameud et al. [20], this current work addresses the problem of attitude synchronization with zero final angular velocity of a set of RB and seeks to extend the findings to incorporate event-triggered communication among the agents. The research aims to explore the feasibility and effectiveness of achieving attitude synchronization while employing event-triggered communication protocols. The communication topology among the agents is represented by a connected and undirected graph. This graph serves as a model for capturing the interconnections and information flow within the MAS.

This article presents two significant contributions. Firstly, a decentralized consensus control algorithm is proposed based on quaternions when communication is limited. The algorithm enables each agent to share its state with its neighbors, determined by the communication graph, only when an event occurs. The shared state is stored in memory and utilized in the control law until the occurrence of another event. This approach helps to reduce communication requirements while ensuring stability properties. Furthermore, the article proposes an effortless event-triggered function that ensures local asymptotic stability. The function is independently activated in each agent using local information. This approach reduces the frequency of communication among agents, which can be helpful in practical scenarios such as a network of satellites or aerial robots with limited bandwidth. Also, the proposed distributed control strategy guarantees practical stability, meaning that the system trajectories converge to a ball centered on the origin of the state space error, despite external disturbances.

The rest of the document is structured as follows. Section II presents the mathematical elements used in this study, including quaternions, the dynamic model of the system, graph theory, the event-triggering function definition, and the problem statement. Next, in Section III, the design of the decentralized event-triggered control algorithm is introduced. A set of numerical simulations is performed to validate the proposed algorithm, and the results are presented and discussed thoroughly in Section IV. Finally, in Section V, the main contributions of this work are summarized and provide future research directions.

II. PRELIMINARIES

A. UNIT QUATERNION

In this work, rotations will be represented by unit quaternions that consider the following right-handed coordinate frames: the inertial coordinate frame $\mathbf{E}^f = [\hat{\mathbf{e}}_1^f, \hat{\mathbf{e}}_2^f, \hat{\mathbf{e}}_3^f]$, located at some point in the force-free space, and the coordinate frame associated with the i-th RB denoted by $\mathbf{E}^i = [\hat{\mathbf{e}}_1^i, \hat{\mathbf{e}}_2^i, \hat{\mathbf{e}}_3^i]$, where $i \in \{1, 2, \ldots, N\}$, N is the number of RB in the system, and $\hat{\mathbf{e}}_1^i, \hat{\mathbf{e}}_2^i, \hat{\mathbf{e}}_3^i$ are the unit vectors of the coordinate frame $\mathbf{E}^i$.

According to Euler's theorem, the rotation of the i-th RB can be parameterized in terms of a rotation angle $\beta_i \in [-\pi, \pi]$ around a unit vector $\hat{\mathbf{e}}_i \in \mathbb{R}^3$. Therefore, a unit rotation quaternion can be denoted by [43]:

$$\mathbf{Q}_i := \begin{pmatrix} \cos\frac{\beta_i}{2} \\ \hat{\mathbf{e}}_i \sin\frac{\beta_i}{2} \end{pmatrix} = \begin{pmatrix} q_i \\ \mathbf{q}_i \end{pmatrix} \in \mathbb{Q}_u, \tag{1}$$

where $q_i \in \mathbb{R}$, $\mathbf{q}_i \in \mathbb{R}^3$ and $\mathbb{Q}_u = \{\mathbf{Q}_i \in \mathbb{R}^4 \mid \|\mathbf{Q}_i\| = 1\}$. The product of two unit quaternions will be used here to describe the attitude error (relative attitude) that quantifies the difference between two specific attitudes, that is

- If $\mathbf{Q}_i$ defines the current attitude of the i-th RB and $\mathbf{Q}_d$ the desired attitude, the difference between these attitudes is quantified by

$$\tilde{\mathbf{Q}}_i = \mathbf{Q}_d^{-1} \odot \mathbf{Q}_i = \begin{pmatrix} \tilde{q}_i & \tilde{\mathbf{q}}_i^T \end{pmatrix}^T, \tag{2}$$

  where $\mathbf{Q}_d^{-1} = \begin{pmatrix} q_d & -\mathbf{q}_d^T \end{pmatrix}^T$ is the conjugate of the quaternion $\mathbf{Q}_d$. Thus, when the attitude of the i-th agent coincides with the desired attitude, $\mathbf{Q}_d = \mathbf{Q}_i$, then $\tilde{\mathbf{Q}}_i = \begin{pmatrix} \pm 1 & \mathbf{0}^T \end{pmatrix}^T$.
- The relative attitude between the i-th and j-th agents is given by:

$$\mathbf{Q}_{ij} = \mathbf{Q}_j^{-1} \odot \mathbf{Q}_i = \begin{pmatrix} q_{ij} & \mathbf{q}_{ij}{}^T \end{pmatrix}^T. \tag{3}$$

B. ATTITUDE DYNAMICS OF RIGID BODIES

According to the attitude dynamics of the i-th agent, which in this case is an RB, rotating at angular velocity $\boldsymbol{\omega}_i$ with respect to its frame $\mathbf{E}^i$, expressed in the inertial frame $\mathbf{E}^f$, the following set of differential equations is obtained:

$$\Sigma_{R_i} := \begin{cases} \dot{\mathbf{Q}}_i = \frac{1}{2}\begin{pmatrix} -\mathbf{q}_i^T \\ \mathbf{I}_3 q_i + [\mathbf{q}_i^\times] \end{pmatrix} \boldsymbol{\omega}_i \\ \mathbf{J}_i \dot{\boldsymbol{\omega}}_i = -[\boldsymbol{\omega}_i^\times]\mathbf{J}_i\boldsymbol{\omega}_i + \boldsymbol{\Gamma}_i + \boldsymbol{\Gamma}_i^d, \end{cases} \tag{4}$$

where $\mathbf{J}_i$ is the inertia matrix expressed in $\mathbf{E}^i$, $\boldsymbol{\Gamma}_i$ are the torques generated by the actuators around their principal axes, which at the same time, constitute the control input vector, and $\boldsymbol{\Gamma}_i^d$ represents the external disturbance torque vector.

Figure 1 shows a representation of a MAS consisting of a group of RB and their respective reference frames $\mathbf{E}^i$ and $\mathbf{E}^f$.

Thus, assuming that $\mathbf{Q}_d$ is a constant attitude, the rate of change of the error quaternions $\tilde{\mathbf{Q}}_i$ and $\mathbf{Q}_{ij}$ is given by:

$$\begin{aligned} \dot{\tilde{\mathbf{Q}}}_i &= \frac{1}{2}\begin{pmatrix} -\tilde{\mathbf{q}}_i^T \\ \mathbf{I}_3\tilde{q}_i + [\tilde{\mathbf{q}}_i^\times] \end{pmatrix} \boldsymbol{\omega}_i, \\ \dot{\mathbf{Q}}_{ij} &= \frac{1}{2}\begin{pmatrix} -\mathbf{q}_{ij}^T \\ \mathbf{I}_3 q_{ij} + \left[\mathbf{q}_{ij}^\times\right] \end{pmatrix} \boldsymbol{\omega}_{ij}, \end{aligned} \tag{5}$$

with $\boldsymbol{\omega}_{ij} = \boldsymbol{\omega}_i - \boldsymbol{\omega}_j$

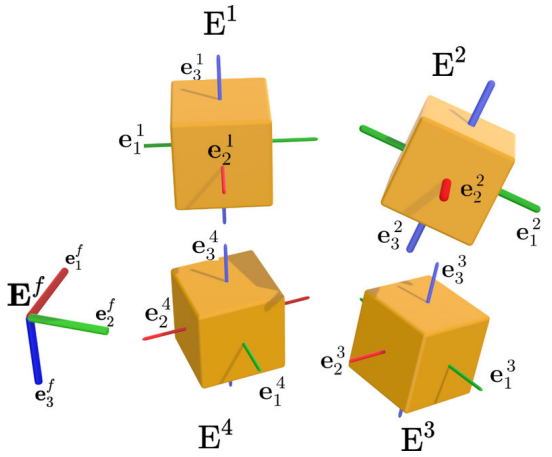

FIGURE 1. Representation of a MAS with their respective reference frames.

C. GRAPH THEORY

Graph theory can be used to define both the communication topology of a multi-agent system and, from a control perspective, establish its stability properties.

Definitions: Consider the graph $\mathcal{G} = \{\mathcal{V}, \mathcal{E}\}$ consisting of a set of nodes $\mathcal{V} = \{1, \ldots, N\}$ and a set of links $\mathcal{E}$ between the nodes i and j, written as $\mathcal{E} = \{(i, j) \in \mathcal{V} \times \mathcal{V}\}$. The nodes (i, j) have the characteristic of being non-adjacent or adjacent. $\mathcal{G}$ is called undirected or bidirectional if $(i, j) \in \mathcal{E} \Leftrightarrow (j, i) \in \mathcal{E}$, and otherwise, the graph is directed. A path from i to j is a sequence of different nodes, starting from i and ending with j, such that each pair of consecutive nodes is adjacent. If there is a path from i to j, then i and j are called connected. If all pairs of nodes in $\mathcal{G}$ are connected and $\mathcal{G}$ is undirected, then one has a strongly connected graph. For bidirectional graphs, the term *strongly* is omitted.

In this research, the following are mainly used: the adjacency matrix A, which is defined by the weights $a_{ij} > 0$ if i and j are adjacent and $a_{ij} = 0$ otherwise, while $a_{ij} = 1$ if the weights are not relevant. The distance $d(i, j)$ between two nodes is the number of links on the shortest path from i to j. The diameter d_{max} of $\mathcal{G}$ is the maximum distance $d(i, j)$ over all pairs of nodes. The degree matrix D of $\mathcal{G}$ is the diagonal matrix with elements d_i equal to the cardinality of the neighbor set $N_i = \{j \in \mathcal{E}\}$ of the node i.

In addition, for the case of a leader-follower array, the Laplacian matrix $\mathcal{L}$ of $\mathcal{G}$ is used, which is defined as $\mathcal{L} = D - A$, where for connected graphs, $\mathcal{L}$ has exactly one eigenvalue equal to zero, and the eigenvalues can be listed in decreasing order $0 = \lambda_1(\mathcal{G}) < \lambda_2(\mathcal{G}) \leq \ldots \leq \lambda_N(\mathcal{G})$. $\bar{\mathcal{G}}$ represents the graph that contains the graph $\mathcal{G}$ and the leader [18].

Let us consider a group of N elements of RB systems or MAS interconnected according to the weighted undirected graph $\mathcal{G}$. Therefore, the following results in the synchronization of RB must be considered.

Lemma 1 (A. Abdessameud and A. Tayebi [20]): Given the set of equations:

$$\sum_{j \in \mathcal{N}_i} a_{ij} \mathbf{q}_{ij} = 0 \quad \text{for } i \in \mathcal{V}, \tag{6}$$

where $a_{ij} \geq 0$ is the ij-entry of the adjacency matrix of $\mathcal{G}$, and $\mathbf{q}_{ij}$ is the vector part of the unit quaternion $\mathbf{Q}_{ij}$, and if the communication graph is a tree, then the only solution to (6) is $\mathbf{q}_{ij} = 0$. Furthermore, if the scalar part q_i of the unit quaternion $\mathbf{Q}_i$ representing the attitude of the i-th rigid body, is strictly positive (or strictly negative), then also $\mathbf{q}_{ij} = 0$ is the only solution to (6) for any undirected graph $\mathcal{G}$.

Lemma 2 (A. Abdessameud and A. Tayebi [20]): Given the set of equations:

$$k_i^p \tilde{\mathbf{q}}_i + \sum_{j \in \mathcal{N}_i} a_{ij} \mathbf{q}_{ij} = 0 \quad \text{for } i \in \mathcal{V}, \tag{7}$$

where $\tilde{\mathbf{q}}_i$ and $\mathbf{q}_{ij}$ are the vector parts of $\tilde{\mathbf{Q}}_i$ and $\mathbf{Q}_{ij}$ respectively, k_i^p is a strictly positive gain scalar, and a_{ij} is defined as in Lemma 1 and if

$$k_i^p > 2 \sum_{j \in \mathcal{N}_i} a_{ij} \quad \text{for } i \in \mathcal{V}, \tag{8}$$

then, the unique solution of (7) is $\tilde{\mathbf{q}}_i = 0$. Furthermore, if the scalar part $\tilde{q}_i$ of the unit quaternion $\tilde{\mathbf{Q}}_i$ representing the attitude of the i-th rigid body is strictly positive, then the previous result holds without any condition on the gains.

Remark 1: The result in Lemma 1 was first presented in [44]. A similar result to the Lemma 2 has been used in [45], [46], [47], [48], and [49]

D. EVENT-TRIGGERED COMMUNICATION IN MAS

Let $\mathcal{G}$ be a graph that describes a dynamic system of the RB type with N nodes, and let a global state vector $x_i = (x_1^T \cdot \cdot \cdot x_N^T)^T$ describe the dynamic evolution of each of the nodes according to the equations:

$$\dot{x}_i = f(x_i, u_i), \tag{9}$$

where, $x_i \in \chi \subset \mathbb{R}^n$ and $u_i \in \mathcal{U} \subset \mathbb{R}^p$.

The transmission of information between agents based on events can be described using two main functions [30]:

- **An event function**: $\bar{e}_i : \chi \times \chi \to \mathbb{R}$, which indicates whether it is necessary for agent i to transmit ($\bar{e}_i > 0$) its state to agent j or not to transmit it ($\bar{e}_i \leq 0$). The event function takes as input the current value of the state x_i, and the value that corresponds to the last time $\bar{e}_i$ was positive whose value has been stored in memory m_i.
- **A distributed control function based on memory**: the control function $u_i(m_i, m_j)$ depends on the memories of the states x_i and x_j. This means that the control of the agent i depends on the state transmitted by the agent i the last time an event occurred and the state coming from the agent j. It should be noted that since the event function depends on the current state x_i of the agent i, this state also affects the control function. The characteristic that the control is distributed is because the control of the agent i only depends on the set $N_i \subset \mathcal{V}$ that describes the graph.

E. PROBLEM STATEMENT

This work considers a group of RB (e.g., satellites, drones, submarines, manipulator robots, among others) spatially distributed and connected through a MAS-type communication network. Each agent shares information only with neighboring agents. The topology of the communication network is represented by an undirected and connected graph, i.e., there is a path between each of the agents of the graph and communication in both directions with $N_i \subset \mathcal{V}$. The leader agent, which is not affected by any agent in the network, is established as an autonomous system and will be responsible for generating the desired final attitude with zero angular velocity. In addition, it is assumed that there is at least one agent in the network that can have access to the reference dictated by the leader agent. In the proposed control scheme, an event function will determine the instant when the i-th agent must transmit its attitude (quaternion) and angular velocity to the j-th neighboring agent or agents.

Consequently, the objective of this work is to design a control law to achieve alignment to a reference attitude $\mathbf{Q}_d$ with final angular velocity $\boldsymbol{\omega}_i = 0$, starting from any initial condition $\mathbf{Q}_i(0)$ and $\boldsymbol{\omega}_i(0)$.

III. DISTRIBUTED CONTROL WITH EVENT-TRIGGERED COMMUNICATION

In this section, we describe the event-triggered control design for the MAS with the associated RB dynamics described by equation (4). To do this, we establish the following definitions:

Definition 1: $\mathbf{Q}_i^m$, $\mathbf{Q}_j^m$ and $\boldsymbol{\omega}_i^m$, $\boldsymbol{\omega}_j^m$ for $i \in \mathcal{V}$ and $j \in \mathcal{N}_i$, are the quaternion and angular velocity, respectively, of the i-th and j-th RB the last time an event occurred. The superscript m indicates that such a value is maintained as a memory.

Definition 2: $\mathbf{Q}_{ij}^m = (\mathbf{Q}_i^m)^{-1} \odot \mathbf{Q}_j^m = \left(q_{ij}^m \ \mathbf{q}_{ij}^{m\,T}\right)^T$ and $\boldsymbol{\omega}_i^m - \boldsymbol{\omega}_j^m$ are the relative attitude and the angular velocity difference between the i-th and j-th RB, respectively. The superscript m indicates the same as the previous definition.

Definition 3: $\mathbf{Q}_i^e = \left(\mathbf{Q}_i^m\right)^{-1} \odot \mathbf{Q}_i = \left(q_i^e \ \mathbf{q}_i^{e\,T}\right)^T$ represents the relative attitude between the current attitude of the i-th rigid body and its attitude the last time an event occurred. Furthermore,

$$\mathbf{Q}_i^e := \begin{pmatrix} \cos\frac{\beta_i^e}{2} \\ \hat{\mathbf{e}}_i \sin\frac{\beta_i^e}{2} \end{pmatrix} = \begin{pmatrix} q_i^e \\ \mathbf{q}_i^e \end{pmatrix} \in \mathbb{Q}_u, \tag{10}$$

Now we are in a position to state the main result.

Proposition 1: Consider a MAS of N elements of RB with dynamics given by equation (4) that can interact under a flow of information described by $\mathcal{G}$. In addition, assume that there is a virtual leader with a constant desired attitude $\mathbf{Q}_d$. If there is communication between the leader and the i-th agent, then there exist constants $K_0^p, D_i > 0$ such that the distributed control function based on events can be defined as:

$$\Gamma_i = -K_0^p \tilde{\mathbf{q}}_i - D_i \boldsymbol{\omega}_i - \sum_{j \in \mathcal{N}_i} a_{ij} \left(\mathbf{q}_{ij}^m + \alpha \left(\boldsymbol{\omega}_i^m - \boldsymbol{\omega}_j^m \right) \right), \tag{11}$$

where the parameter $\alpha > 0$ and $a_{ij} > 0$ for $i \in \mathcal{V}$ and $j \in N_i$ synchronize the attitude of the RB to the desired attitude $\mathbf{Q}_d$.

The event function is given by:

$$\bar{e}_i = \left|\beta_i^e\right| - \beta_0, \tag{12}$$

with $\beta_i^e = 2\arccos(q_i^e)$ and β_0 being the activation threshold for the event function.

The proof of Proposition 1 is given in Appendix. However, to keep the practical motivation of this work, please remember that the main aspects of the control strategy are:

1) The control $\boldsymbol{\Gamma}_i$ defined in equation (11) is composed of two terms

$$\Gamma_i = \underbrace{-k_0^p \tilde{\mathbf{q}}_i - D_i \boldsymbol{\omega}_i}_{\boldsymbol{\Gamma}_i^1 := \text{local}} \underbrace{- \sum_{j \in \mathcal{N}_i} a_{ij} \left(\mathbf{q}_{ij}^m + \alpha \left(\boldsymbol{\omega}_i^m - \boldsymbol{\omega}_j^m \right) \right)}_{\boldsymbol{\Gamma}_i^2 := \text{distributed}},$$

   - $\boldsymbol{\Gamma}_i^1$ is considered a local control term and k_0^p is a positive constant that will be different from zero if and only if the i-th agent has direct communication with the leader, who dictates the constant desired attitude $\mathbf{Q}_d$. D_i is a positive constant for the i-th agent.
   - $\boldsymbol{\Gamma}_i^2$ is considered a distributed control term and is calculated with the value in memory of the state of the i-th and j-th agent.
2) The event function in equation (12) depends on the attitude quaternion of the i-th agent and denoted $\mathbf{Q}_i$, as well as the value $\mathbf{Q}_i^m$ of the quaternion in memory the last time an event occurred and which was transmitted to the neighboring agents according to the communication graph.
3) When such event function satisfies $\bar{e}_i > 0$, the state of the i-th agent $(\mathbf{Q}_i, \boldsymbol{\omega}_i)$ is saved as a memory $(\mathbf{Q}_i^m, \boldsymbol{\omega}_i^m)$ and in turn transmitted to the neighboring agents according to the communication topology dictated by the graph $\mathcal{G}$. In addition, $\boldsymbol{\Gamma}_i^2$ is calculated with the updated data at each new event. Otherwise, the state $(\mathbf{Q}_i, \boldsymbol{\omega}_i)$ is not transmitted, the memories are not updated, and the control is calculated with the memories saved the last time the event occurred.

Figure 2 illustrates the block diagram of the control system corresponding to each agent.

IV. SIMULATION RESULTS

Numerical simulations were carried out to validate the proposed control strategy. Specifically, four agents established as undirected graph $\mathcal{G}$ shown in Fig. 3 is the communication topology.

Accordingly, agent 1 has information about the virtual leader (VL), and each agent obeys the RB dynamics given by equation (4). For this computer experiment, it was assumed that the four RBs are identical. However, if the RBs were not identical, the control strategy is still valid since it does not depend on the RBs' parameters.

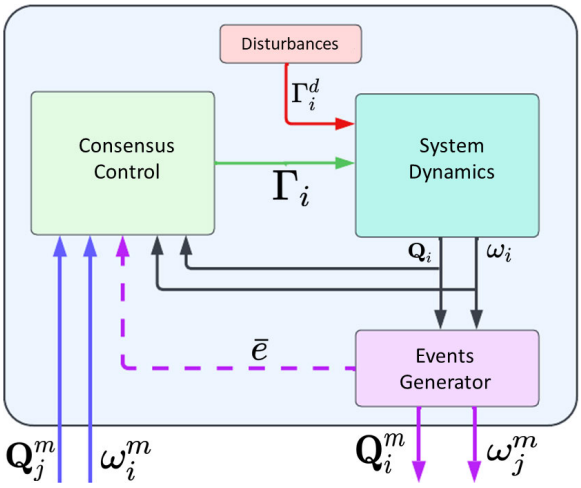

FIGURE 2. Block diagram of the control system for each agent.

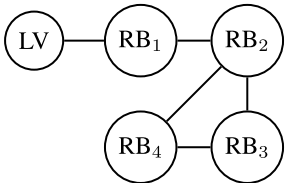

FIGURE 3. Communication graph between the RBs.

TABLE 1. Simulation parameters.

Parameter	Description	Value	Units
J_x	Inertia in x-axis	$10.95 \times 10^{-}6$	$\mathrm{kg \cdot m^2}$
J_y	Inertia in y-axis	$11.02 \times 10^{-}6$	$\mathrm{kg \cdot m^2}$
J_z	Inertia in z-axis	$21.12 \times 10^{-}6$	$\mathrm{kg \cdot m^2}$
K_0^p	Gain	100	-
D_i	Gain	8	-
a_{ij}	Adjacency matrix element	1	-
α	Gain	1	-
β_0	Threshold	0.01	rad

TABLE 2. Rigid body initial conditions.

Agent	Attitude (quaternion)				Angular velocity (rad/s)		
	q_0	q_1	q_2	q_3	ω_x	ω_y	ω_z
RB_1	0.937	0.193	0.217	0.193	1	0	0.5
RB_2	0.843	0.340	0.415	0.021	0.5	0.1	0
RB_3	0.923	0.006	0.227	0.308	0.3	0.3	0.3
RB_4	0.735	-0.21	0.491	0.415	1	0.5	1

Table 1 displays all parameters used in the MATLAB/Simulink program: the threshold values for the event function (12), the gain control values for equation (11), and the elements of the inertia matrix for each RB in (4) are considered to be a diagonal matrix which corresponds to a small agent like a commercial quadrotor or a CubeSat [50].

Initial conditions (IC), both for attitude and angular velocity for each agent, are shown in Table 2. Where q_0 is the scalar part of the quaternion of attitude and q_1, q_2 and q_3 are the corresponding components of the vector part. Whilst, $\boldsymbol{\omega}_x$, $\boldsymbol{\omega}_y$ and $\boldsymbol{\omega}_z$ are the components of the angular velocity.

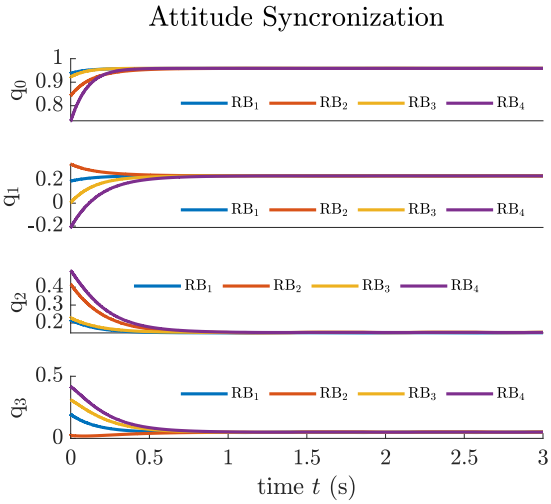

FIGURE 4. Attitude synchronization without disturbances.

Simulations considered two scenarios: in the first one, there were no external disturbances in the agents, i.e., $\Gamma_i^d = 0$ for $i \in \mathcal{V}$, while in the second scenario, disturbances were affecting the agents of the network. In both cases, the physical parameters of the agents, the control gains, and the initial conditions were the same.

The reader is invited to visualize an animation of the implementation of the strategy, which is found at the link https://bit.ly/IEEE-Sim-video and where the execution of the simulations in MATLAB/Simulink is observed together with the 3D-Animation toolbox.

A. SCENARIO 1: ATTITUDE SYNCHRONIZATION WITHOUT DISTURBANCES

The attitude synchronization of the MAS is performed by applying the distributed control and the events function, defined by equations (11) and (12), respectively. The results for each component of the quaternion for each agent are shown in Figure 4. It can be observed that the agents reached the same attitude, i.e., the synchronization occurred successfully in less than a second.

In Figure 5, the evolution in time of the normalized angular velocity for each of the four agents is shown. It can be observed that a successful synchronization occurred, as well as the expected zero final angular velocity.

The attitude errors in terms of $\beta_i^e = 2 \arccos q_i^e$ for each agent are shown in Figure 6. It can be observed that the attitude errors are smaller than 1×10^{-3} rad after the synchronization occurred. Accordingly, to literature, in applications like interferometry [51], satellite networks [22], or fractionated spacecraft [23], this magnitude is considered acceptable.

In Figure 7, the evolution in time of the event function $\bar{e}_i$ is shown. It can be observed that the frequency of events is significantly reduced over time as each agent synchronizes with the group. The total number of events generated by each agent is $\bar{e} = \{72, 238, 148, 259\}$. Note that the agent connected to the virtual leader is the one that generates the

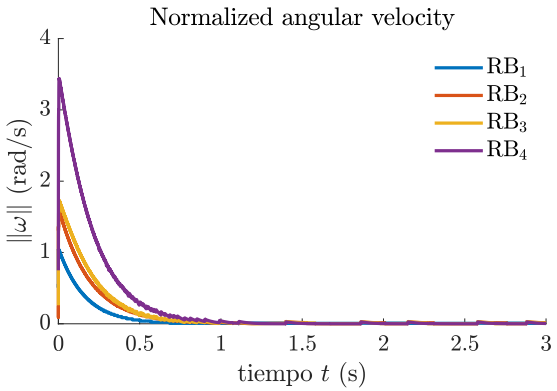

FIGURE 5. Angular velocity without disturbances.

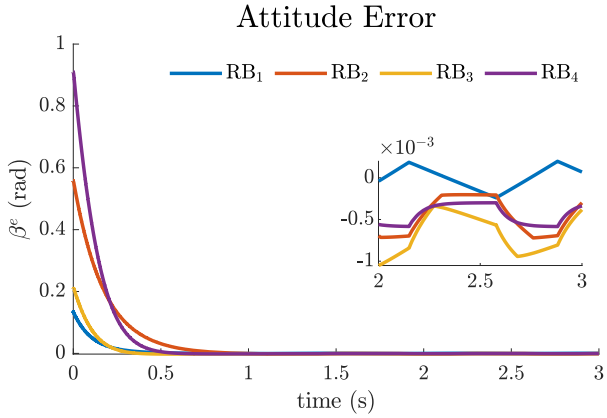

FIGURE 6. Attitude errors without disturbances.

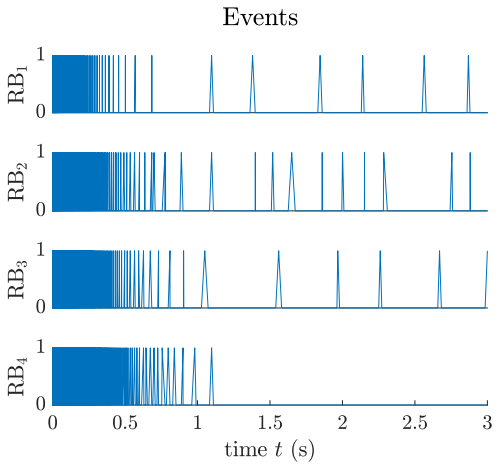

FIGURE 7. Events without disturbances.

least events due to its immediate reaction to being connected directly to the leader, as expected.

B. SCENARIO 2: ATTITUDE SYNCHRONIZATION WITH EXTERNAL DISTURBANCES

In this second scenario, the disturbance is a pulse applied to the control signal of agent RB_1, which is applied from the beginning in the form sine wave, $d = 0.5\sin(2\pi t)$.

The results for each component of the quaternion for each agent are shown in Figure 8. In this case, it can be observed

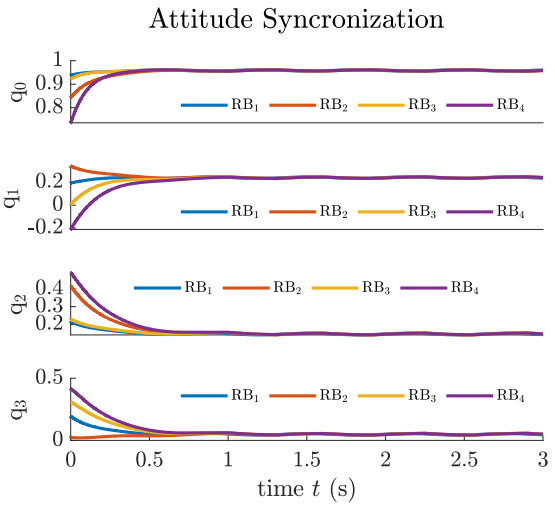

FIGURE 8. Attitude synchronization with disturbances.

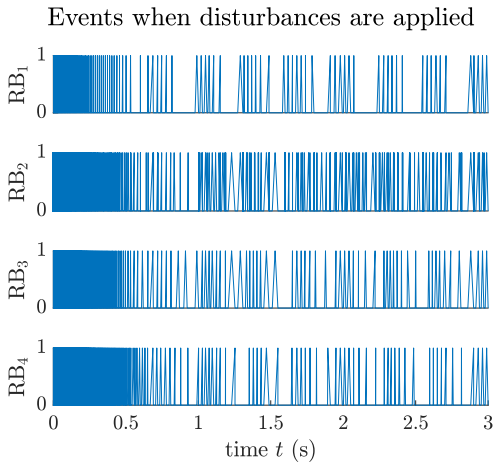

FIGURE 9. Events with disturbances.

the system can compensate for the disturbance, and the agents synchronize at the same time as in the previous scenario.

In Figure 9, the evolution in time of the event function $\bar{e}_i$ is shown. The number of events generated by each agent is $\bar{e} = \{118,\ 394,\ 199,\ 313\}$. Due to the disturbance, the number of events generated by the agents is higher than in the previous scenario.

C. COMPARISON OF TWO APPROACHES: CLASSICAL SCHEME AND EVENT-BASED COMMUNICATION SCHEME

In this epigraph, a comparison is made between a ''classical'' scheme, where communication between the agents of the network is carried out continuously in time, and the modern scheme proposed in this work, where communication is activated only when it is necessary according to the event function.

For this purpose, we will denote $\mathbf{Q}_i^E$ the quaternion that represents the attitude of the i-th agent under an event-based communication scheme without disturbances and $\mathbf{Q}_i^C$ the quaternion that represents the attitude of the i-th agent under a continuous communication scheme. An analysis of the

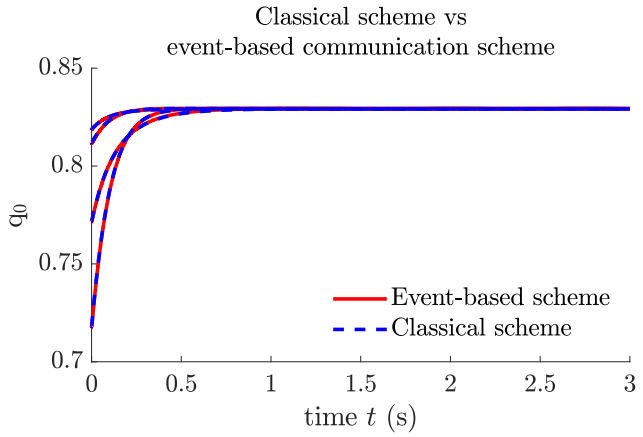

FIGURE 10. Comparison of synchronization: classical scheme vs. event-based communication scheme.

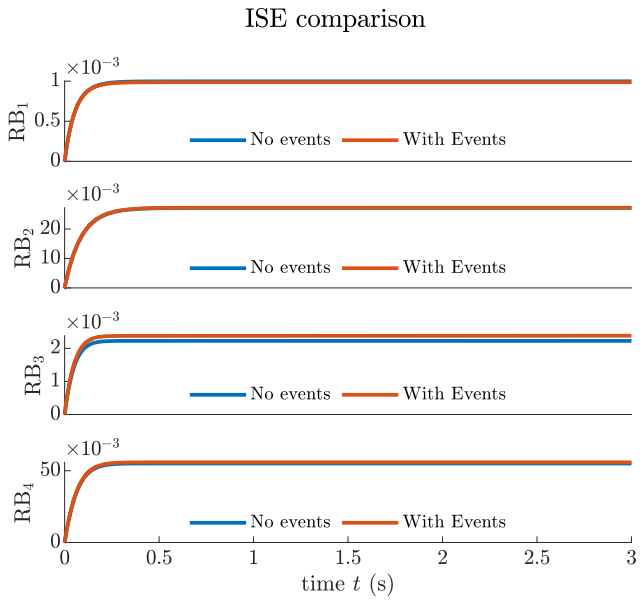

FIGURE 11. Comparison of ISE.

synchronization of the agents is carried out using the error of attitude between both scenarios of control, which is determined by: $\mathbf{Q}_i^{EC} = \left(\mathbf{Q}_i^E\right)^{-1} \odot \mathbf{Q}_i^C = \left(\, q_i^{EC} \;\; -(\mathbf{q}_i^{EC})^T \,\right)^T$.

For the analysis of the error of attitude, the index of performance ISE (Integrated Squared Error) proposed in [52] was used:

$$ISE = \int_0^{t_f} \bar{\beta}_i^{EC}(t)^2 \, dt, \tag{13}$$

where $\bar{\beta}_i^{EC}(t) = \arccos q_i^{EC}(t)$ is the error metric.

Figure 10 shows the evolution in time of the scalar components of $\mathbf{Q}_i^E$ and $\mathbf{Q}_i^C$ for the four agents of the network. As we can see, the behavior of the agents is very similar in both approaches. This is more clearly visible in Figure 11, where the ISE is shown for each agent. It can be observed that the sacrifice in precision is negligible using the event-based communication scheme.

V. CONCLUSION

In this article, a consensus control with event-triggered communication for a multi-agent system has been presented. Quaternions are used to represent the attitude of the agents. The control algorithm presented is useful in scenarios where the agents of the system are unable to maintain continuous communication since only state updates are required when the event function is activated.

The event function is designed in a decentralized way so that each agent independently transmits information and only when necessary, i.e., when the value of the error in the states of the agent is greater than a given threshold.

The decentralized consensus control allows each agent to reach synchronization with the group based on its own states and the states of its neighbors stored in the memory of the last time there was an event.

The results obtained from the study indicate that the proposed control algorithm achieves attitude synchronization among the networked agents in less than a second. The achieved synchronization error is reported to be below 10^{-3} rad (radians). While such an error value may be negligible for applications like drone flying formations, its acceptability for spacecraft applications depends on factors such as mission requirements, instrument sensitivity, and operational constraints. Although 10^{-3} rad might be acceptable for certain spacecraft missions, it may not meet the precision demands of others, especially those involving precise pointing accuracy, high-resolution imaging, or scientific measurements with strict error tolerances.

Moreover, the proposed control algorithm can compensate for the disturbances applied to the control signal of the agents, and the amount of events is reduced as the group synchronizes. In addition, The article also presents a comparison of performance indices between continuous communication and communication triggered by events.

APPENDIX
STABILITY PROOF

In this appendix, the proof of the stability of the system is presented. Before starting the proof, let us recall the following variables:

$$\begin{aligned}
\mathbf{Q}_i^e &= \left(\mathbf{Q}_i^m\right)^{-1} \odot \mathbf{Q}_i \\
\mathbf{Q}_j^e &= \left(\mathbf{Q}_j^m\right)^{-1} \odot \mathbf{Q}_j \\
\hat{\mathbf{Q}}_i &= \mathbf{Q}_d^{-1} \odot \mathbf{Q}_i^m
\end{aligned}$$

We can express $\mathbf{Q}_{ij}^m$ in terms of the defined variables as follows:

$$\begin{aligned}
\mathbf{Q}_{ij}^m &= \left(\mathbf{Q}_j^m\right)^{-1} \odot \mathbf{Q}_i^m \\
&= \left(\mathbf{Q}_j^e \odot \mathbf{Q}_j^{-1}\right) \odot \mathbf{Q}_i \odot (\mathbf{Q}_i^e)^{-1} \\
&= \mathbf{Q}_j^e \odot \left(\mathbf{Q}_j^{-1} \odot \mathbf{Q}_i\right) \odot (\mathbf{Q}_i^e)^{-1} \\
&= \mathbf{Q}_j^e \odot \mathbf{Q}_{ij} \odot (\mathbf{Q}_i^e)^{-1} \\
&= \mathbf{Q}_{ij} \otimes \mathbf{Q}_j^e \odot (\mathbf{Q}_i^e)^{-1}.
\end{aligned} \tag{14}$$

Now, let us define:

$$\bar{\mathbf{Q}}_{ij}^{e} = \mathbf{Q}_{j}^{e} \odot (\mathbf{Q}_{i}^{e})^{-1}. \tag{15}$$

Then:

$$\mathbf{Q}_{ij}^{m} = \mathbf{Q}_{ij} \otimes \bar{\mathbf{Q}}_{ij}^{e} = \bar{\mathbf{Q}}_{ij}^{e} \odot \mathbf{Q}_{ij}. \tag{16}$$

$$\mathbf{Q}_{ij}^{m} = \begin{pmatrix} q_{ij}^{e} & -\left[\mathbf{q}_{ij}^{e}\right]^{T} \\ \mathbf{q}_{ij}^{e} & \mathbf{I}_{3} q_{ij}^{e} + \left[\mathbf{q}_{ij}^{e}\right]^{\times} \end{pmatrix} \begin{pmatrix} q_{ij} \\ \mathbf{q}_{ij} \end{pmatrix} \tag{17}$$

Therefore, $\mathbf{q}_{ij}^{m}$ is:

$$\mathbf{q}_{ij}^{m} = q_{ij}\mathbf{q}_{ij}^{e} + \left(\mathbf{I}_{3} q_{ij}^{e} + \left[\mathbf{q}_{ij}^{e}\right]^{\times}\right) \mathbf{q}_{ij}. \tag{18}$$

Assuming $\beta_{ij}^{e} \approx 0$, we have:

$$\begin{aligned} \mathbf{q}_{ij}^{e} &\approx \hat{\mathbf{e}}_{ij} \frac{\beta_{ij}^{e}}{2}, \quad q_{ij}^{e} \approx 1, \\ \mathbf{q}_{ij}^{m} &\approx \mathbf{q}_{ij} + \hat{\mathbf{e}}_{ij} \frac{\beta_{ij}^{e}}{2} q_{ij} + \hat{\mathbf{e}}_{ij} \frac{\beta_{ij}^{e\,\times}}{2} \mathbf{q}_{ij}. \end{aligned} \tag{19}$$

Proof: Considering the Lyapunov candidate function, $V : \mathbb{R}^3 \times \mathbb{Q}_u \times \mathbb{Q}_u \to \mathbb{R}$ defined as:

$$V = \sum_{i=1}^{N} \left(\frac{1}{2} \boldsymbol{\omega}_i^T J_i \boldsymbol{\omega}_i + 2K_0^p \left(1 - \tilde{\mathbf{q}}_i\right) + \sum_{j \in N_i} a_{ij} \left(1 - \mathbf{q}_{ij}\right) \right) \tag{20}$$

Recall that N is the number of agents in the set $\mathcal{V}$ and $\mathcal{N}_i$ is the set of neighbors of the i-th agent. Note that the function V is positive definite. The derivative of (20) along the trajectories of (4) is given by:

$$\begin{aligned} \dot{V} &= \sum_{i=1}^{N} \left(\boldsymbol{\omega}_i^T J_i \dot{\boldsymbol{\omega}}_i - 2K_0^p \dot{\tilde{\mathbf{q}}}_i - \sum_{j \in N_i} a_{ij} \dot{\mathbf{q}}_{ij} \right) \\ &= \sum_{i=1}^{n} \left(\dot{V}_1 + \dot{V}_2 + \dot{V}_3 \right), \end{aligned} \tag{21}$$

where

$$\begin{aligned} \dot{V}_1 &= \boldsymbol{\omega}_i^T \Gamma_i, \\ \dot{V}_2 &= -K_0^p \tilde{\mathbf{q}}_i^T \boldsymbol{\omega}_i, \\ \dot{V}_3 &= -\frac{1}{2} \sum_{j \in N_i} a_{ij} \mathbf{q}_{ij}^T \boldsymbol{\omega}_{ij}. \end{aligned} \tag{22}$$

Substituting $\boldsymbol{\Gamma}_i$ given by (11) we obtain:

$$\begin{aligned} \dot{V} = \sum_{i=1}^{N} \Bigg(\boldsymbol{\omega}_i^T \Bigg(& -K_0^p \tilde{\mathbf{q}}_i - D_i \boldsymbol{\omega}_i \\ & - \sum_{j \in N_i} a_{ij} \left(\mathbf{q}_{ij}^m + \alpha \left(\boldsymbol{\omega}_i^m - \boldsymbol{\omega}_j^m \right) \right) \Bigg) \Bigg) \\ & + \dot{V}_2 + \dot{V}_3. \end{aligned} \tag{23}$$

The error between the memory of the angular velocity vector (the value of the angular velocity vector the last time an event occurred) and the current value of the angular velocity of the i-th and j-th agent is given by:

$$\begin{aligned} e_{\boldsymbol{\omega}_i} &= \boldsymbol{\omega}_{ij}^m - \boldsymbol{\omega}_i \Rightarrow \boldsymbol{\omega}_i^m = \boldsymbol{\omega}_i + e_{\boldsymbol{\omega}_i}, \\ e_{\boldsymbol{\omega}_j} &= \boldsymbol{\omega}_j^m - \boldsymbol{\omega}_j \Rightarrow \boldsymbol{\omega}_j^m = \boldsymbol{\omega}_j + e_{\boldsymbol{\omega}_j}. \end{aligned} \tag{24}$$

Consider the second term of the law of control, which can be rewritten by introducing the error variables defined previously:

$$\begin{aligned} & \sum_{j \in N_i} a_{ij} \left(\mathbf{q}_{ij}^m + \alpha \left(\boldsymbol{\omega}_i^m - \boldsymbol{\omega}_j^m \right) \right) \\ & = \sum_{j \in N_i} a_{ij} \Bigg(\mathbf{q}_{ij} + \hat{\mathbf{e}}_{ij} \frac{\beta_{ij}^e}{2} q_{ij} + \left(\hat{\mathbf{e}}_{ij} \frac{\beta_{ij}^{e\,\times}}{2} \right) \mathbf{q}_{ij} \\ & \qquad + \alpha \left(\boldsymbol{\omega}_i + e_{\boldsymbol{\omega}_i} - \boldsymbol{\omega}_j - e_{\boldsymbol{\omega}_j} \right) \Bigg) \\ & = \sum_{j \in N_i} a_{ij} \left(\mathbf{q}_{ij} + \alpha \left(\boldsymbol{\omega}_i - \boldsymbol{\omega}_j \right) \right) + \Delta_i, \end{aligned} \tag{25}$$

where Δ_i is given by:

$$\Delta_i = \sum_{j \in N_i} a_{ij} \left(\hat{\mathbf{e}}_{ij} \frac{\beta_{ij}^e}{2} q_{ij} + \left(\hat{\mathbf{e}}_{ij} \frac{\beta_{ij}^{e\,\times}}{2} \right) \mathbf{q}_{ij} + \alpha \left(e_{\boldsymbol{\omega}_i} - e_{\boldsymbol{\omega}_j} \right) \right) \tag{26}$$

In consequence, (23) can be written as:

$$\begin{aligned} \dot{V} = \sum_{i=1}^{N} \Bigg(& -K_0^p \boldsymbol{\omega}_i^T \tilde{\mathbf{q}}_i - D_i \boldsymbol{\omega}_i^T \boldsymbol{\omega}_i - \sum_{j \in N_i} a_{ij} \boldsymbol{\omega}_i^T \mathbf{q}_{ij} \\ & - \alpha \sum_{j \in N_i} a_{ij} \boldsymbol{\omega}_i^T \boldsymbol{\omega}_{ij} + K_0^p \tilde{\mathbf{q}}_i^T \boldsymbol{\omega}_i \\ & + \frac{1}{2} \sum_{j \in N_i} a_{ij} \mathbf{q}_{ij}^T \boldsymbol{\omega}_{ij} + \boldsymbol{\omega}_i^T \Delta_i \Bigg) \end{aligned} \tag{27}$$

with $\boldsymbol{\omega}_{ij} = \boldsymbol{\omega}_i - \boldsymbol{\omega}_j$, besides, is possible to show that [19]:

$$\sum_{i=1}^{N} \sum_{j \in N_i} a_{ij} \boldsymbol{\omega}_i^T \mathbf{q}_{ij} = \frac{1}{2} \sum_{i=1}^{N} \sum_{j \in N_i} a_{ij} \mathbf{q}_{ij}^T \boldsymbol{\omega}_{ij}, \tag{28}$$

$$\alpha \sum_{i=1}^{N} \sum_{j \in N_i} a_{ij} \boldsymbol{\omega}_i^T \boldsymbol{\omega}_{ij} = \alpha \sum_{i=1}^{N} \sum_{j \in N_i} a_{ij} \left\| \boldsymbol{\omega}_i - \boldsymbol{\omega}_j \right\|^2, \tag{29}$$

simplifying (27) to:

$$\begin{aligned} \dot{V} = & - \sum_{i=1}^{N} D_i \boldsymbol{\omega}_i^T \boldsymbol{\omega}_i - \alpha \sum_{i=1}^{N} \sum_{j \in N_i} a_{ij} \left\| \boldsymbol{\omega}_i - \boldsymbol{\omega}_j \right\|^2 \\ & + \sum_{i=1}^{N} \boldsymbol{\omega}_i^T \Delta_i, \end{aligned} \tag{30}$$

then, applying Young's inequality to the last term:

$$\sum_{i=1}^{N} \boldsymbol{\omega}_i^T \Delta_i \leq \sum_{i=1}^{N} \mu \boldsymbol{\omega}_i^T \boldsymbol{\omega}_i + \sum_{i=1}^{N} \frac{1}{4\mu} \Delta_i^T \Delta_i, \tag{31}$$

substituting this inequality into the previous expression and rearranging the terms:

$$\begin{aligned} \dot{V} \leq & -\sum_{i=1}^{N} D_i \boldsymbol{\omega}_i^T \boldsymbol{\omega}_i - \alpha \sum_{i=1}^{N} \sum_{j \in N_i} a_{ij} \left\| \boldsymbol{\omega}_i - \boldsymbol{\omega}_j \right\|^2 \\ & + \sum_{i=1}^{N} \mu \boldsymbol{\omega}_i^T \boldsymbol{\omega}_i + \sum_{i=1}^{N} \frac{1}{4\mu} \Delta_i^T \Delta_i, \end{aligned} \tag{32}$$

a new constant $\kappa = D_i - \mu$ is defined and substituted into the equation:

$$\begin{aligned} \dot{V} \leq & -\sum_{i=1}^{N} \kappa \boldsymbol{\omega}_i^T \boldsymbol{\omega}_i - \alpha \sum_{i=1}^{N} \sum_{j \in N_i} a_{ij} \left\| \boldsymbol{\omega}_i - \boldsymbol{\omega}_j \right\|^2 \\ & + \sum_{i=1}^{N} \frac{1}{4\mu} \Delta_i^T \Delta_i, \end{aligned} \tag{33}$$

simplifying and rearranging the terms, we have:

$$\begin{aligned} \dot{V} \leq & -\sum_{i=1}^{N} \kappa \left\| \boldsymbol{\omega}_i \right\|^2 - \alpha \sum_{i=1}^{N} \sum_{j \in N_i} a_{ij} \left\| \boldsymbol{\omega}_i - \boldsymbol{\omega}_j \right\|^2 \\ & + \sum_{i=1}^{N} \frac{1}{4\mu} \left\| \Delta_i \right\|^2, \end{aligned} \tag{34}$$

To have $\dot{V} \leqslant 0$ it must be satisfied the following:

$$\left\| \boldsymbol{\omega}_i \right\| \geqslant \frac{1}{2\sqrt{\mu\kappa}} \left\| \Delta_i \right\|. \tag{35}$$

Rewriting Δ_i from (26), we have:

$$\begin{aligned} \Delta_i &= \Delta_j^e + \Delta_i^e, \\ \Delta_j^e &= \sum_{j \in N_i} a_{ij} \left(\hat{\mathbf{e}}_{ij} \frac{\beta_{ij}^e}{2} q_{ij} + \left(\hat{\mathbf{e}}_{ij} \frac{\beta_{ij}^e}{2} \right)^{\times} \mathbf{q}_{ij} - \alpha e_{\boldsymbol{\omega}_j} \right) \\ \Delta_i^e &= \alpha N e_{\boldsymbol{\omega}_i}. \end{aligned} \tag{36}$$

We have:

$$\begin{aligned} \left\| \boldsymbol{\omega}_i \right\| &\geqslant \frac{1}{2\sqrt{\mu\kappa}} \left\| \Delta_j^e + \Delta_i^e \right\| \\ &\geqslant \frac{1}{2\sqrt{\mu\kappa}} \left\| \Delta_j^e \right\| - \frac{1}{2\sqrt{\mu\kappa}} \left\| \Delta_i^e \right\|. \end{aligned} \tag{37}$$

In terms of $\boldsymbol{\omega}_i^m$ and $\boldsymbol{\omega}_i$, we have the following:

$$\left\| \boldsymbol{\omega}_i \right\| + \frac{\alpha N}{2\sqrt{\mu\kappa}} \left\| \boldsymbol{\omega}_i^m - \boldsymbol{\omega}_i \right\| \geqslant \frac{1}{2\sqrt{\mu\kappa}} \left\| \Delta_j^e \right\|. \tag{38}$$

If $\boldsymbol{\omega}_i$ and $\boldsymbol{\omega}_i^m$ satisfy the condition (38) then $\dot{V} \leqslant 0$ and $\boldsymbol{\omega}_i$ is bounded.

On the other hand, recalling that:

$$\mathbf{Q}_{ij}^m = \mathbf{Q}_{ij} \otimes \mathbf{Q}_{ij}^e = \mathbf{Q}_{ij} \otimes \mathbf{Q}_j^e \odot (\mathbf{Q}_i^e)^{-1}, \tag{39}$$

it is possible to find that:

$$\mathbf{Q}_i^e = \left(\mathbf{Q}_{ij}^m \right)^{-1} \odot \mathbf{Q}_{ij} \otimes \mathbf{Q}_j^e, \tag{40}$$

and also recalling that $\mathbf{Q}_i^e = \left(\mathbf{Q}_i^m \right)^{-1} \odot \mathbf{Q}_i$ is the error between the quaternion $\mathbf{Q}_i$ at time t and the memory quaternion $\mathbf{Q}_i^m$, that is, the quaternion the last time there was an event. Now it is easy to identify that $\mathbf{Q}_{ij}^e = \left(\mathbf{Q}_{ij}^m \right)^{-1} \odot \mathbf{Q}_{ij}$. Therefore, right after an event, $\mathbf{Q}_{ij}^e = (1 \; 0^T)^T$ so that:

$$\mathbf{Q}_i^e = \begin{pmatrix} q_i^e \\ \mathbf{q}_i^e \end{pmatrix} = \begin{pmatrix} \cos\left(\frac{\beta_i^e}{2} \right) \\ \hat{\mathbf{e}}_i \sin\left(\frac{\beta_i^e}{2} \right) \end{pmatrix} = \begin{pmatrix} q_j^e \\ \mathbf{q}_j^e \end{pmatrix} \tag{41}$$

which allows writing:

$$\beta_i^e = \underbrace{2 \cos^{-1}\left(q_i^e \right)}_{\beta_0}, \tag{42}$$

β_0 is a tuning parameter and will be tuned by the designer; then, while the condition $\left| \beta_i^e \right| - \beta_0 \leq 0$ is satisfied with β_0 sufficiently small, we have:

$$\mathbf{Q}_{ij}^e \approx \begin{pmatrix} 1 \\ 0 \end{pmatrix} \approx \begin{pmatrix} q_{ij}^e \\ \mathbf{q}_{ij}^e \end{pmatrix} \tag{43}$$

This allows to generate the event function and define the set:

$$\Omega_{\mathbf{Q}} = \left\{ \mathbf{Q}_{ij} \mid \left| \beta_i^e \right| - \beta_0 \leq 0 \right\}. \tag{44}$$

If the quaternion $\mathbf{Q}_{ij}$ belongs to the set $\Omega_{\mathbf{Q}}$, then we can approximate $\mathbf{Q}_{ij}^e$ as $\begin{pmatrix} 1 \\ 0 \end{pmatrix} \approx \begin{pmatrix} q_{ij}^e \\ \mathbf{q}_{ij}^e \end{pmatrix}$, which implies that $\mathbf{q}_{ij}^e = 0$. Additionally, we have $\mathbf{Q}_{ij}^m = \mathbf{Q}_{ij}$, leading to $\dot{\mathbf{Q}}_{ij} = \begin{pmatrix} 0 \\ 0 \end{pmatrix}$, which further implies $\boldsymbol{\omega}_{ij} = 0$. Consequently, we have $\left\| \boldsymbol{\omega}_i - \boldsymbol{\omega}_j \right\| = 0$. As a result, $e_{\boldsymbol{\omega}_j} = 0$, and we can express it as:

$$\Delta_j^e = \sum_{j \in N_i} a_{ij} \left(\hat{\mathbf{e}}_{ij} \frac{\beta_{ij}^e}{2} q_{ij} + \left(\hat{\mathbf{e}}_{ij} \frac{\beta_{ij}^e}{2} \right)^{\times} \mathbf{q}_{ij} - \alpha e_{\boldsymbol{\omega}_j} \right) = 0. \tag{45}$$

Going back to the Lyapunov function within the set $\boldsymbol{\Omega}_{\mathbf{Q}}$, it is now that:

$$\dot{V} = -\sum_{i=1}^{n} \kappa \boldsymbol{\omega}_i^T \boldsymbol{\omega}_i \leq 0. \tag{46}$$

Now we have to find the largest invariant set such that:

$$\tilde{\mathbf{q}}_i = 0, \quad \mathbf{q}_{ij} = 0, \quad \dot{V} = 0, \tag{47}$$

$\dot{V} = 0$ leads to $\boldsymbol{\omega}_i = 0$.

Going back firstly to the system in a closed loop, we have that:

$$\begin{aligned} \dot{\mathbf{Q}}_i &= \frac{1}{2} \begin{pmatrix} -\mathbf{q}_i^T \\ \mathbf{I}_3 q_i + [\mathbf{q}_i^{\times}] \end{pmatrix} \boldsymbol{\omega}_i \\ \mathbf{J}_i \dot{\boldsymbol{\omega}}_i &= -[\boldsymbol{\omega}_i^{\times}] \mathbf{J}_i \boldsymbol{\omega}_i + \boldsymbol{\Gamma}_i. \end{aligned} \tag{48}$$

There are two cases to consider:

- **Case a)** When the agent is connected to the leader:

$$\mathbf{\Gamma} i = -k_0^p \tilde{\mathbf{q}}_i - D_i \boldsymbol{\omega} i - \sum_{i=1}^{n} a_{ij} \left(\mathbf{q}_{ij}^m + \alpha \left(\boldsymbol{\omega}_i^m - \boldsymbol{\omega}_j^m \right) \right). \tag{49}$$

- **Case b)** When the agent does not have a direct connection with the leader:

$$\mathbf{\Gamma}_i = - \sum_{i=1}^{n} a_{ij} \left(\mathbf{q}_{ij}^m + \alpha \left(\boldsymbol{\omega}_i^m - \boldsymbol{\omega}_j^m \right) \right) \tag{50}$$

Now, let's analyze the closed-loop system for each case:

- **Case a)**
  Recalling that the system evolves in $\Omega_{\mathbf{Q}}$, we have $\mathbf{Q}_{ij} = \mathbf{Q}_{ij}^m$ and $\boldsymbol{\omega}_i^m - \boldsymbol{\omega}_j^m = 0$.
  Thus, we obtain:

$$0 = \mathbf{\Gamma}_i \Rightarrow 0 = -k_0^p \tilde{\mathbf{q}}_i - \sum_{i=1}^{n} a_{ij} \mathbf{q}_{ij}. \tag{51}$$

  By Lemma 2, the only solution is $\tilde{\mathbf{q}}_i = 0$.
- **Case b)**
  We have:

$$0 = \mathbf{\Gamma}_i \Rightarrow 0 = - \sum_{i=0}^{n} a_{ij} \mathbf{q}_{ij}. \tag{52}$$

  By Lemma 1, the only solution is $\mathbf{q}_{ij} = 0$.

The previous results show that while the state of the i-th agent is in the set $\Omega_{\mathbf{Q}}$, it is neither necessary to update the value of the state in the control law nor to transmit the state of the i-th agent to the neighboring agents contained in the set N_i. In the opposite case, *i.e.*, when $\mathbf{Q}_i$ or $\boldsymbol{\omega}_i$ or both, leave the set $\Omega_{\mathbf{Q}}$, which occurs when the condition given by (12) is fulfilled, it will be necessary to update the control law and transmit the state to the neighboring agents. This ends the proof.

REFERENCES

[1] H. Song, D. B. Rawat, S. Jeschke, and C. Brecher, "Front matter," in *Cyber-Physical Systems, Intelligent Data-Centric Systems*. Boston, MA, USA: Academic Press, 2017.

[2] R. Olfati-Saber and R. M. Murray, "Consensus problems in networks of agents with switching topology and time-delays," *IEEE Trans. Autom. Control*, vol. 49, no. 9, pp. 1520–1533, Sep. 2004.

[3] N. Ahmed, J. Cortes, and S. Martinez, "Distributed control and estimation of robotic vehicle networks: Overview of the special issue—Part II," *IEEE Control Syst.*, vol. 36, no. 4, pp. 18–21, Apr. 2016.

[4] A. Okubo, "Dynamical aspects of animal grouping: Swarms, schools, flocks, and herds," *Adv. Biophys.*, vol. 22, pp. 1–94, Jan. 1986.

[5] M. A. Akhloufi, A. Couturier, and N. A. Castro, "Unmanned aerial vehicles for wildland fires: Sensing, perception, cooperation and assistance," *Drones*, vol. 5, no. 1, p. 15, Feb. 2021.

[6] J. Zhang, X. Yue, H. Zhang, and T. Xiao, "Optimal unmanned ground vehicle—Unmanned aerial vehicle formation-maintenance control for air-ground cooperation," *Appl. Sci.*, vol. 12, no. 7, p. 3598, Apr. 2022.

[7] M. Mammarella, L. Comba, A. Biglia, F. Dabbene, and P. Gay, "Cooperative agricultural operations of aerial and ground unmanned vehicles," in *Proc. IEEE Int. Workshop Metrology for Agricult. Forestry (MetroAgriFor)*, Nov. 2020, pp. 224–229.

[8] J. Kim, "Cooperative localisation for deep-sea exploration using multiple unmanned underwater vehicles," *IET Radar, Sonar Navigat.*, vol. 14, no. 8, pp. 1244–1248, Aug. 2020.

[9] L. Sun, "Adaptive fault-tolerant constrained control of cooperative spacecraft rendezvous and docking," *IEEE Trans. Ind. Electron.*, vol. 67, no. 4, pp. 3107–3115, Apr. 2020.

[10] B. Hichri, J.-C. Fauroux, L. Adouane, I. Doroftei, and Y. Mezouar, "Design of cooperative mobile robots for co-manipulation and transportation tasks," *Robot. Comput.-Integr. Manuf.*, vol. 57, pp. 412–421, Jun. 2019.

[11] B. Jiang, Q. Hu, and M. I. Friswell, "Fixed-time attitude control for rigid spacecraft with actuator saturation and faults," *IEEE Trans. Control Syst. Technol.*, vol. 24, no. 5, pp. 1892–1898, Sep. 2016.

[12] Q. Hu, B. Jiang, and Y. Zhang, "Observer-based output feedback attitude stabilization for spacecraft with finite-time convergence," *IEEE Trans. Control Syst. Technol.*, vol. 27, no. 2, pp. 781–789, Mar. 2019.

[13] W. Koch, R. Mancuso, R. West, and A. Bestavros, "Reinforcement learning for UAV attitude control," *ACM Trans. Cyber-Phys. Syst.*, vol. 3, no. 2, pp. 1–21, Apr. 2019.

[14] P. Razzaghi, E. Al Khatib, and Y. Hurmuzlu, "Swarm control of magnetically actuated millirobots," 2021, *arXiv:2111.03931*.

[15] D. Milutinovic and P. Lima, "Modeling and optimal centralized control of a large-size robotic population," *IEEE Trans. Robot.*, vol. 22, no. 6, pp. 1280–1285, Dec. 2006.

[16] L. Bakule, "Decentralized control: Status and outlook," *Annu. Rev. Control*, vol. 38, no. 1, pp. 71–80, 2014.

[17] L. Bakule and M. Papík, "Decentralized control and communication," *Annu. Rev. Control*, vol. 36, no. 1, pp. 1–10, Apr. 2012.

[18] F. L. Lewis, H. Zhang, K. Hengster-Movric, and A. Das, *Cooperative Control of Multi-Agent Systems: Optimal and Adaptive Design Approaches*. Berlin, Germany: Springer, 2013.

[19] W. Ren and R. W. Beard, *Distributed Consensus in Multi-Vehicle Cooperative Control*. Berlin, Germany: Springer, 2008.

[20] A. Abdessameud and A. Tayebi, *Motion Coordination for VTOL Unmanned Aerial Vehicles: Attitude Synchronisation and Formation Control*. Berlin, Germany: Springer, 2013.

[21] H. Du, M. Z. Q. Chen, and G. Wen, "Leader-following attitude consensus for spacecraft formation with rigid and flexible spacecraft," *J. Guid., Control, Dyn.*, vol. 39, no. 4, pp. 944–951, Apr. 2016.

[22] F. Guo and S. Zhang, "Event-triggered coordinated attitude method for chip satellite cluster," *Acta Astronautica*, vol. 160, pp. 451–460, Jul. 2019.

[23] C. Wang, L. Guo, C. Wen, Q. Hu, and J. Qiao, "Event-triggered adaptive attitude tracking control for spacecraft with unknown actuator faults," *IEEE Trans. Ind. Electron.*, vol. 67, no. 3, pp. 2241–2250, Mar. 2020.

[24] C. Xu, B. Wu, X. Cao, and Y. Zhang, "Distributed adaptive event-triggered control for attitude synchronization of multiple spacecraft," *Nonlinear Dyn.*, vol. 95, no. 4, pp. 2625–2638, Mar. 2019.

[25] X. Jin, Y. Shi, Y. Tang, and X. Wu, "Event-triggered attitude consensus with absolute and relative attitude measurements," *Automatica*, vol. 122, Dec. 2020, Art. no. 109245.

[26] B. Wu, C. Xu, and Y. Zhang, "Decentralized adaptive control for attitude synchronization of multiple spacecraft via quantized information exchange," *Acta Astronautica*, vol. 175, pp. 57–65, Oct. 2020.

[27] B. Wu, "Spacecraft attitude control with input quantization," *J. Guid., Control, Dyn.*, vol. 39, no. 1, pp. 176–181, Jan. 2016.

[28] P. Shi, H. Wang, and C.-C. Lim, "Network-based event-triggered control for singular systems with quantizations," *IEEE Trans. Ind. Electron.*, vol. 63, no. 2, pp. 1230–1238, Feb. 2016.

[29] B. Wu, Q. Shen, and X. Cao, "Event-triggered attitude control of spacecraft," *Adv. Space Res.*, vol. 61, no. 3, pp. 927–934, Feb. 2018.

[30] J.-F. Guerrero-Castellanos, A. Vega-Alonzo, S. Durand, N. Marchand, V. Gonzalez-Diaz, J. Castañeda-Camacho, and W.-F. Guerrero-Sánchez, "Leader-following consensus and formation control of VTOL-UAVs with event-triggered communications," *Sensors*, vol. 19, no. 24, pp. 1–26, 2019.

[31] C. Zhang, J. Wu, M.-Z. Dai, B. Li, and M. Wang, "Event- and self-triggered control of attitude coordination to multi-spacecraft system," *Aircr. Eng. Aerosp. Technol.*, vol. 92, no. 7, pp. 1085–1092, Jun. 2020.

[32] F.-Q. Di, A.-J. Li, Y. Guo, C.-Q. Xie, and C.-Q. Wang, "Event-triggered sliding mode attitude coordinated control for spacecraft formation flying system with disturbances," *Acta Astronautica*, vol. 188, pp. 121–129, Nov. 2021.

[33] C. Wang, L. Guo, C. Wen, X. Yu, and J. Huang, "Attitude coordination control for spacecraft with disturbances and event-triggered communication," *IEEE Trans. Aerosp. Electron. Syst.*, vol. 57, no. 1, pp. 586–596, Feb. 2021.
[34] N. Marchand, S. Durand, and J. F. G. Castellanos, "A general formula for event-based stabilization of nonlinear systems," *IEEE Trans. Autom. Control*, vol. 58, no. 5, pp. 1332–1337, May 2013.
[35] J. F. Guerrero-Castellanos, J. J. Téllez-Guzmán, S. Durand, N. Marchand, J. U. Alvarez-Muñoz, and V. R. González-Díaz, "Attitude stabilization of a quadrotor by means of event-triggered nonlinear control," *J. Intell. Robotic Syst.*, vol. 73, nos. 1–4, pp. 123–135, Jan. 2014.
[36] M. Miskowicz, *Event-Based Control and Signal Processing*. Boca Raton, FL, USA: CRC Press, 2015.
[37] D. Xie, S. Xu, B. Zhang, Y. Li, and Y. Chu, "Consensus for multi-agent systems with distributed adaptive control and an event-triggered communication strategy," *IET Control Theory Appl.*, vol. 10, no. 13, pp. 1547–1555, 2016.
[38] E. Aranda-Escolástico, M. Guinaldo, R. Heradio, J. Chacon, H. Vargas, J. Sánchez, and S. Dormido, "Event-based control: A bibliometric analysis of twenty years of research," *IEEE Access*, vol. 8, pp. 47188–47208, 2020.
[39] D. V. Dimarogonas, E. Frazzoli, and K. H. Johansson, "Distributed event-triggered control for multi-agent systems," *IEEE Trans. Autom. Control*, vol. 57, no. 5, pp. 1291–1297, May 2012.
[40] G. S. Seyboth, D. V. Dimarogonas, and K. H. Johansson, "Event-based broadcasting for multi-agent average consensus," *Automatica*, vol. 49, no. 1, pp. 245–252, Jan. 2013.
[41] E. Garcia, Y. Cao, and D. W. Casbeer, "Decentralized event-triggered consensus with general linear dynamics," *Automatica*, vol. 50, no. 10, pp. 2633–2640, Oct. 2014.
[42] C. Nowzari, E. Garcia, and J. Cortés, "Event-triggered communication and control of networked systems for multi-agent consensus," *Automatica*, vol. 105, pp. 1–27, Jul. 2019.
[43] F. Landis Markley and J. L. Crassidis, *Fundamentals of Spacecraft Attitude Determination and Control*. Berlin, Germany: Springer, 2014.
[44] A. Abdessameud and A. Tayebi, "Attitude synchronization of a group of spacecraft without velocity measurements," *IEEE Trans. Autom. Control*, vol. 54, no. 11, pp. 2642–2648, Nov. 2009.
[45] A. Abdessameud and A. Tayebi, "Decentralized attitude alignment control of spacecraft within a formation without angular velocity M," in *Proc. 17th World Congr., Int. Fed. Automatic Control*, 2008, pp. 1766–1771.
[46] A. Abdessameud and A. Tayebi, "Attitude synchronization of a spacecraft formation without velocity measurement," in *Proc. 47th IEEE Conf. Decis. Control*, Dec. 2008, pp. 3719–3724.
[47] A. Abdessameud and A. Tayebi, "On the coordinated attitude alignment of a group of spacecraft without velocity measurements," in *Proc. 48h IEEE Conf. Decis. Control (CDC) Held Jointly, 28th Chin. Control Conf.*, Dec. 2009, pp. 1476–1481.
[48] H. Bai, M. Arcak, and J. T. Wen, "Rigid body attitude coordination without inertial frame information," *Automatica*, vol. 44, no. 12, pp. 3170–3175, Dec. 2008.
[49] W. Ren, "Distributed attitude alignment in spacecraft formation flying," *Int. J. Adapt. Control Signal Process.*, vol. 21, nos. 2–3, pp. 95–113, 2007.
[50] J. Li, M. Post, T. Wright, and R. Lee, "Design of attitude control systems for CubeSat-class nanosatellite," *J. Control Sci. Eng.*, vol. 2013, pp. 1–15, Jan. 2013.
[51] N. K. Lincoln, "Multi agent control for space based interferometry," Ph.D. thesis, School Eng. Sci., Univ. Southampton, Southampton, U.K., 2009.
[52] R. N. Clark, "Integral of the error squared as a performance index for automatic control systems," *Trans. Amer. Inst. Electr. Eng., II, Appl. Ind.*, vol. 79, no. 6, pp. 467–471, Jan. 1961.

JUAN R. AYALA-OLIVARES received the B.S. degree in mechatronics engineering from Universidad Tecnológica de Tlaxcala, Tlaxcala, Mexico, in 2012, and the M.S. degree in electronics engineering from Instituto Nacional de Astrofísica, Óptica y Electrónica, Puebla, Mexico, in 2018, where he is currently pursuing the Ph.D. degree in electronics engineering.

His research interests include nonlinear control, multi-agent systems, embedded systems, and robotics.

ROGERIO ENRÍQUEZ-CALDERA received the B.S. degree in physics from Universidad Nacional Autónoma de México, Mexico City, Mexico, in 1982, and the M.Sc. degree in theoretical physics and mathematics and the Ph.D. degree in electrical engineering in communications from the University of New Brunswick, New Brunswick, Canada, in 1989 and 1994, respectively.

He is currently a Professor with Instituto Nacional de Astrofísica, Óptica y Electrónica, Puebla, Mexico, and he collaborates with the UN specifically with the Regional Center for Space Science and Technology Education for Latin America and the Caribbean (CRECTEALC) promoting international research projects mainly with Europe (Switzerland and Greece). His research in the area of space has allowed him to define the curriculum of the unique postgraduate program in space science and technology in Mexico, for which he has structured the academy of professors with national (INAOE) and international members. As part of this graduate program, he is in charge of the Simulation Laboratory for Flight Simulation in Formation (SimVFF Laboratory), INAOE, as well as the GNSS research area. His research interests include mathematical models of satellite receivers, the definition of Mexican standards in the area of technology, virtual libraries, geomatics, and satellite positioning and navigation.

J. FERMI GUERRERO-CASTELLANOS (Member, IEEE) received the B.Sc. degree in electronics from Benemérita Universidad Autónoma de Puebla (BUAP), Mexico, in 2002, the M.Sc. degree in automatic control from the Grenoble Institute of Technology, in 2004, and the Ph.D. degree in automatic control from Université Grenoble Alpes (former Joseph Fourier University), France, in 2008.

From January 2008 to June 2008, he was a Postdoctoral Researcher with the GIPSA-Lab Laboratory, Grenoble, France. After spending one year with the University Polytechnic of Puebla, Mexico, as an Assistant Professor, he joined the Faculty of Electronics, BUAP, in 2009, as a Full Professor, where he established and currently heads the Control and Autonomous Systems Laboratory. His research interests include modeling and control of mechatronics and unmanned vehicles, inertial navigation systems, event-based control, multi-agent systems, active-disturbance rejection control, and renewable energy applications.

SYLVAIN DURAND received the M.Sc.Eng. degree in control and embedded systems from Grenoble-INP, in 2007, and the Ph.D. degree in systems and control theory from the University of Grenoble, Grenoble, France, in 2011.

He is currently an Associate Professor with INSA Strasbourg and the ICube Laboratory, Strasbourg, France. His research interests include event-based control and control of embedded cyber-physical and robotic systems with limited resources.